PTEP

Prog. Theor. Exp. Phys. **2016**, 053D02 (23 pages)
DOI: 10.1093/ptep/ptw055

Spin-polarized versus chiral condensate in quark matter at finite temperature and density

Hiroaki Matsuoka[1], Yasuhiko Tsue[2,*,†], João da Providência[3,†], Constança Providência[3,†], Masatoshi Yamamura[4,†], and Henrik Bohr[5,†]

[1]*Graduate School of Integrated Arts and Science, Kochi University, Kochi 780-8520, Japan*
[2]*Physics Division, Faculty of Science, Kochi University, Kochi 780-8520, Japan*
[3]*CFisUC, Departamento de Física, Universidade de Coimbra, 3004-516 Coimbra, Portugal*
[4]*Department of Pure and Applied Physics, Faculty of Engineering Science, Kansai University, Suita 564-8680, Japan*
[5]*Department of Physics, B.307, Danish Technical University, DK-2800 Lyngby, Denmark*
*E-mail: tsue@kochi-u.ac.jp

Received January 7, 2016; Revised February 29, 2016; Accepted April 10, 2016; Published May 24, 2016

It is shown that the spin-polarized condensate appears in quark matter at high baryon density and low temperature due to the tensor-type four-point interaction in the Nambu–Jona-Lasinio-type model as a low-energy effective theory of quantum chromodynamics. It is indicated within this low-energy effective model that the chiral symmetry is broken again by the spin-polarized condensate on increasing the quark number density, while chiral symmetry restoration occurs, in which the chiral condensate disappears at a certain density.

Subject Index D30

1. Introduction

One of the recent topics of interest in the physics of the strong interaction, namely, in the physics governed by quantum chromodynamics (QCD), has been to clarify the structure of the phase diagram on the plane with respect to baryon chemical potential and temperature (see, e.g., Ref. [1]). In the region of finite temperature and zero baryon chemical potential, lattice QCD simulation works and reliable calculations based on first principles have been performed until now. However, in the region of low temperature and finite baryon chemical potential, the possibility of various phases, such as the color superconducting phase [2–4], quarkyionic phase [5], inhomogeneous chiral-condensed phase [6–8], and so on, has been indicated.

In heavy-ion collision experiments such as the relativistic heavy-ion collider (RHIC) experiment, it is believed that the quark–gluon phase is realized. Also, in the large hadron collider (LHC) experiment, it is expected that more extreme states of QCD with finite temperature and density and/or a strong magnetic field may be created in the quark–gluon phase. It is interesting to understand what phases arise under extreme conditions. The quark–gluon phase under extreme conditions may be realized in the inner core of compact stars such as neutron stars, magnetars, and quark stars, if they exist. Therefore, the investigation of quark matter at low temperature and high density is also important to understand compact star objects.

[†]These authors contributed equally to this work.

In our previous papers, it has been shown that a spin-polarized phase may appear and be realized instead of the color superconducting phase in cases of both two [9] and three flavors [10] in the region with finite quark chemical potential at zero temperature. It is also interesting to investigate possible phases in the region with high density and low temperature from the viewpoint of the physics of compact stars, in particular, the structure of the inner cores of compact stars. It has also been shown in our recent work [11] that there is a possibility of the existence of a strong magnetic field on the surface of compact stars if there exists a quark spin-polarized phase, which leads to the spontaneous magnetization of quark matter due to the anomalous magnetic moment of the quark, while only symmetric quark matter has been considered. If spin polarization really leads to spontaneous magnetization in the mechanism developed in the previous paper [11], it is a possible candidate for the origin of the strong magnetic field in so-called magnetars [12–14].

In this paper, which follows Refs. [15] and [9], the possibility of the quark spin-polarized phase is investigated in the region of finite quark chemical potential and finite temperature by using the Nambu–Jona-Lasinio (NJL) model [16–19] with the tensor-type four-point interaction between quarks [20], instead of the pseudovector-type four-point interaction [21,22]. As for the tensor-type four-point interaction, this interaction term was also introduced to investigate meson spectroscopy, in particular for vector and axial-vector mesons [23]. As another application, the dynamic properties of vector mesons were investigated in the extended NJL model including the tensor-type interaction [24]. Also, the chiral condensate and the quark spin polarization, namely, the tensor condensate, are considered simultaneously in the case with only one flavor instead of the color superconductor [25].

This paper is organized as follows: In the next section, a recapitulation of the NJL model with the tensor-type four-point interaction between quarks is given; in this model, the chiral condensate and quark spin-polarized condensate are considered simultaneously. In Sect. 3, the thermodynamic potential at zero temperature is introduced under the mean-field approximation. In Sect. 4, the thermodynamic potential at finite temperature and density is given and derived. A derivation of the thermodynamic potential at zero temperature from that at finite temperature is given in Appendix A. Also, the effective potential is evaluated in Appendix B. In Appendix C, the analytic calculation for the thermodynamic potential is presented. In Sect. 5, the numerical results are given through the calculation of the thermodynamic potential under various temperatures and quark chemical potentials. The results are summarized in a phase diagram on the plane with respect to the quark chemical potential and temperature, in which the possible phases, the position of the phase boundary, and the order of the phase transition are shown, apart from the color superconducting phase. In Appendix D, an idea introducing the tensor-type four-point interaction between quarks, which plays an essential role in this paper, is given from the viewpoint of the two-gluon exchange process in QCD. The last section is devoted to a summary and concluding remarks.

2. NJL model with a tensor-type four-point interaction

Let us consider the NJL-model Lagrangian density with a tensor-type four-point interaction. The Lagrangian density with $su(2)$-flavor symmetry can be expressed as

$$\mathcal{L} = \mathcal{L}_0 + \mathcal{L}_{\rm S} + \mathcal{L}_{\rm T}, \tag{2.1}$$

$$\mathcal{L}_0 = \bar{\psi}\left(i\gamma^\mu \partial_\mu - m_0\right)\psi, \tag{2.2}$$

$$\mathcal{L}_{\rm S} = G_S \left\{ \left(\bar{\psi}\psi\right)^2 + \left(\bar{\psi} i\gamma^5 \vec{\tau}\psi\right)^2 \right\}, \tag{2.3}$$

$$\mathcal{L}_{\rm T} = -\frac{G_T}{4} \left\{ \left(\bar{\psi}\gamma^\mu\gamma^\nu\vec{\tau}\psi\right)\cdot\left(\bar{\psi}\gamma_\mu\gamma_\nu\vec{\tau}\psi\right) + \left(\bar{\psi} i\gamma^5\gamma^\mu\gamma^\nu\psi\right)\left(\bar{\psi} i\gamma^5\gamma_\mu\gamma_\nu\psi\right) \right\}, \tag{2.4}$$

where m_0 is the current quark mass for up- and down-quarks and the components of $\vec{\tau}$ are the Pauli matrices for the isospin. It is known that these current quark masses are slightly different for each flavor, but we have used approximately the same value. The first two terms, $\mathcal{L}_0 + \mathcal{L}_{\rm S}$, are the original NJL-model Lagrangian density. In this paper $\mathcal{L}_{\rm T}$ is added into the model, according to the Fierz transform. Then, the spin matrix appears from $\mathcal{L}_{\rm T}$ when $\mu = 1$, $\nu = 2$ or $\mu = 2$, $\nu = 1$ as follows:

$$\Sigma_3 = -i\gamma^1\gamma^2 = \begin{pmatrix} \sigma_3 & 0 \\ 0 & \sigma_3 \end{pmatrix}.$$

Since we use the mean-field approximation, we get the following mean-field Lagrangian density:

$$\begin{aligned} \mathcal{L}_{\rm MFA} = {} & \bar{\psi}\left(i\gamma^\mu\partial_\mu - m_0\right)\psi + G_S\left\{2\left\langle\bar{\psi}\psi\right\rangle\left(\bar{\psi}\psi\right) - \left\langle\bar{\psi}\psi\right\rangle^2\right\} \\ & + \frac{G_T}{2}\left\{2\left\langle\bar{\psi}\Sigma_3\tau_3\psi\right\rangle\left(\bar{\psi}\Sigma_3\tau_3\psi\right) - \left\langle\bar{\psi}\Sigma_3\tau_3\psi\right\rangle^2\right\}, \end{aligned} \tag{2.5}$$

where $\langle\cdots\rangle$ means vacuum expectation value. Here τ_3 is the third component of the Pauli matrix for isospin. When it operates on ψ for the up-quark (down-quark), the matrix changes into 1 (-1) as its eigenvalue. Thus we can safely express $\bar{\psi}\Sigma_3\tau_3\psi$ as follows:

$$\bar{\psi}\Sigma_3\tau_3\psi \longrightarrow \bar{\psi}\Sigma_3\psi\tau_f,$$

where $\tau_f = 1$ (-1) when $f =$ up-quark (down-quark). Let us define the following quantities:

$$F \equiv -G_T\left\langle\bar{\psi}\Sigma_3\psi\right\rangle, \quad M \equiv -2G_S\left\langle\bar{\psi}\psi\right\rangle, \quad M_{\rm q} \equiv m_0 + M.$$

F and M are especially important quantities, because if F and/or M are not equal to zero, then spin polarization and/or chiral condensation occur. Here, $M_{\rm q}$ is just a constituent quark mass. Substituting these quantities into Eq. (2.5), we convert $\mathcal{L}_{\rm MFA}$ into

$$\mathcal{L}_{\rm MFA} = \bar{\psi}\left(i\gamma^\mu\partial_\mu - M_{\rm q}\right)\psi - F\left(\bar{\psi}\Sigma_3\psi\right) - \frac{M^2}{4G_S} - \frac{F^2}{2G_T}. \tag{2.6}$$

Let us switch from the Lagrangian formalism to the Hamiltonian formalism by Legendre transformation. First we must obtain the canonical momentum π_α, $\pi_\alpha = \partial\mathcal{L}_{\rm MFA}/\partial\dot{\psi}_\alpha = i\psi_\alpha^\dagger$, where α means an index for the spinor and isospin. We, therefore, get the Hamiltonian density:

$$\begin{aligned} \mathcal{H}_{\rm MFA} = {} & \pi_\alpha\dot{\psi}_\alpha - \mathcal{L}_{\rm MFA} \\ = {} & \bar{\psi}\left(-i\vec{\gamma}\cdot\vec{\nabla} + M_{\rm q}\right)\psi + F\left(\bar{\psi}\Sigma_3\psi\right) + \frac{M^2}{4G_S} + \frac{F^2}{2G_T}. \end{aligned} \tag{2.7}$$

Thus, the Hamiltonian is expressed as

$$H_{\rm MFA} = \int d^3x\, \psi^\dagger\gamma^0\left(-i\vec{\gamma}\cdot\vec{\nabla} + M_{\rm q} + F\Sigma_3\right)\psi + V\frac{M^2}{4G_S} + V\frac{F^2}{2G_T},$$

where V is the volume of this system. We transform $\psi(x)$ by a Fourier transformation as $\psi(x) = \int d^3p/(2\pi)^3\cdot\tilde{\psi}(p)e^{i\vec{p}\cdot\vec{x}}$. Substituting this into $H_{\rm MFA}$, we obtain

$$H_{\rm MFA} = \int \frac{d^3p}{(2\pi)^3}\tilde{\psi}^\dagger\gamma^0\left(\vec{\gamma}\cdot\vec{p} + M_{\rm q} + F\Sigma_3\right)\tilde{\psi} + V\frac{M^2}{4G_S} + V\frac{F^2}{2G_T}. \tag{2.8}$$

What we must do is to diagonalize $H_{\rm MFA}$. The nondiagonal terms are

$$\begin{aligned} h_{\rm MFA} &\equiv \gamma^0 \left(\vec{\gamma}\cdot\vec{p} + M_{\rm q} + F\Sigma_3\right) \\ &= \begin{pmatrix} F\sigma_3 + M_{\rm q} & \vec{p}\cdot\vec{\sigma} \\ \vec{p}\cdot\vec{\sigma} & -F\sigma_3 - M_{\rm q} \end{pmatrix} \\ &= \begin{pmatrix} F + M_{\rm q} & 0 & p_3 & p_1 - ip_2 \\ 0 & -F + M_{\rm q} & p_1 + ip_2 & -p_3 \\ p_3 & p_1 - ip_2 & -F - M_{\rm q} & 0 \\ p_1 + ip_2 & -p_3 & 0 & F - M_{\rm q} \end{pmatrix}. \end{aligned}$$

Since $h_{\rm MFA}$ is a Hermitian matrix, it is diagonalized by a unitary matrix. The eigenvalues are obtained as

$$\pm E_{\vec{p}}^{(\eta)} = \pm\sqrt{p_3^2 + \left(\sqrt{p_1^2 + p_2^2 + M_{\rm q}^2} + \eta F\right)^2}, \tag{2.9}$$

where $\eta = \pm 1$.

3. Thermodynamic potential at zero temperature

Next, we introduce a quark chemical potential μ and a number density operator $\mathcal{N}$ in order to discuss a finite-density system at zero temperature. The thermodynamic potential is defined as follows:

$$\Phi = \mathcal{H}_{\rm MFA} - \mu\mathcal{N}. \tag{3.1}$$

The next step is to calculate the expectation value. Since we consider the zero-temperature system in this section, the system in which quasiparticles are degenerate is treated. Hence, we must sum over momenta from zero to the single-quasiparticle energy equal to the chemical potential. Sandwiching with a "bra" and "ket", we obtain

$$\begin{aligned} \Phi &= \frac{1}{V}\langle \text{F.D.}|\left(H_{\rm MFA} - \mu\int d^3x\,\mathcal{N}\right)|\text{F.D.}\rangle \\ &= \frac{1}{V}\sum_{\vec{p},\eta,\tau,\alpha}^{E_{\vec{p}}^{(\eta)}\le\mu,\,\vec{p}^2\le\Lambda^2}\left(E_{\vec{p}}^{(\eta)} - \mu\right) + \frac{M^2}{4G_S} + \frac{F^2}{2G_T}, \end{aligned}$$

where $|\text{F.D.}\rangle$ means the degenerate Fermi gas constituted by quasiparticles and Λ is a three-momentum cutoff parameter for the integration over momenta. Here, τ and α are indices for isospin and quark color, respectively. The upper limit of integration is imposed by two conditions, which are $E_{\vec{p}}^{(\eta)} \le \mu$ and $\vec{p}^2 \le \Lambda^2$. We would like to discuss spin polarization and chiral condensate simultaneously. However, the above expression does not have a contribution from the Dirac sea. Since the chiral condensate occurs by the effect of the Dirac sea, we must add its contribution. Thus, we get

$$\Phi(M, F, \mu) = \frac{1}{V}\sum_{\vec{p},\eta,\tau,\alpha}^{E_{\vec{p}}^{(\eta)}\le\mu,\,\vec{p}^2\le\Lambda^2}\left(E_{\vec{p}}^{(\eta)} - \mu\right) - \frac{1}{V}\sum_{\vec{p},\eta,\tau,\alpha}^{\vec{p}^2\le\Lambda^2} E_{\vec{p}}^{(\eta)} + \frac{M^2}{4G_S} + \frac{F^2}{2G_T}, \tag{3.2}$$

where the second term represents the contribution from the Dirac sea (negative energy sea). We change the sum $\frac{1}{V}\sum_{\vec{p}}$ into the integration $\int\frac{d^3p}{(2\pi)^3}$. Then, the thermodynamic potential can

be expressed as

$$\Phi(M, F, \mu) = \Phi_1 + \Phi_2 + \Phi_3 + \Phi_4, \tag{3.3}$$

where

$$\Phi_1(F, M, \mu) = \sum_{\tau,\alpha} \int_{\Gamma_1} \frac{d^3p}{(2\pi)^3} \left\{ \sqrt{p_3^2 + \left(\sqrt{p_1^2 + p_2^2 + M_{\rm q}^2} + F \right)^2} - \mu \right\},$$
$$\Gamma_1 = \left\{ E_{\vec{p}}^{(+1)} \le \mu,\ \vec{p}^2 \le \Lambda^2 \right\} \tag{3.4}$$
$$\Phi_2(M, F, \mu) = \sum_{\tau,\alpha} \int_{\Gamma_2} \frac{d^3p}{(2\pi)^3} \left\{ \sqrt{p_3^2 + \left(\sqrt{p_1^2 + p_2^2 + M_{\rm q}^2} - F \right)^2} - \mu \right\},$$
$$\Gamma_2 = \left\{ E_{\vec{p}}^{(-1)} \le \mu,\ \vec{p}^2 \le \Lambda^2 \right\} \tag{3.5}$$
$$\Phi_3(M, F, \mu) = -\sum_{\eta,\tau,\alpha} \int_{\Gamma_3} \frac{d^3p}{(2\pi)^3} \sqrt{p_3^2 + \left(\sqrt{p_1^2 + p_2^2 + M_{\rm q}^2} + \eta F \right)^2},$$
$$\Gamma_3 = \left\{ \vec{p}^2 \le \Lambda^2 \right\} \tag{3.6}$$
$$\Phi_4(M, F, \mu) = \frac{M^2}{4G_S} + \frac{F^2}{2G_T}. \tag{3.7}$$

Here, $\Phi_i (i = 1, 2, 3, 4)$ means, respectively, the contributions from positive energy for $\eta = +1$, positive energy for $\eta = -1$, vacuum, and the mean field, respectively. $\Gamma_i (i = 1, 2, 3)$ is the domain of integration over momenta. Since these integrands do not depend on τ or α, the summations over τ and α give factors 2 and 3, respectively.

4. Thermodynamic potential at finite temperature and density

We have discussed the thermodynamic potential at zero temperature in the previous section. In this section let us consider the thermodynamic potential at finite temperature. We define a thermodynamic potential at finite temperature, $\Omega(M, F, \mu, T)$, as follows:

$$\Omega\left(M, F, \mu, T\right) \equiv \mathcal{H}'_{\rm MFA} - \mu(\mathcal{N}_{\rm P} - \mathcal{N}_{\rm AP}) + V_{\rm vacuum} - TS, \tag{4.1}$$
$$\mathcal{H}'_{\rm MFA} \equiv \sum_{\vec{p},\eta,\tau,\alpha} E_{\vec{p}}^{(\eta)} \left(n_{\vec{p}}^{(\eta)} + \bar{n}_{\vec{p}}^{(\eta)} \right) + \frac{M^2}{4G_S} + \frac{F^2}{2G_T},$$
$$\mathcal{N}_{\rm P} \equiv \sum_{\vec{p},\eta,\tau,\alpha} n_{\vec{p}}^{(\eta)}, \quad \mathcal{N}_{\rm AP} \equiv \sum_{\vec{p},\eta,\tau,\alpha} \bar{n}_{\vec{p}}^{(\eta)},$$
$$n_{\vec{p}}^{(\eta)} = \frac{1}{1 + \exp\left(\left(E_{\vec{p}}^{(\eta)} - \mu \right) / T \right)}, \qquad \bar{n}_{\vec{p}}^{(\eta)} = \frac{1}{1 + \exp\left(\left(E_{\vec{p}}^{(\eta)} + \mu \right) / T \right)},$$
$$V_{\rm vacuum} \equiv -\sum_{\vec{p},\eta,\tau,\alpha} E_{\vec{p}}^{(\eta)},$$

where T means the temperature of the system and $n_{\vec{p}}^{(\eta)}$ and $\bar{n}_{\vec{p}}^{(\eta)}$ are the distribution functions for the particle and antiparticle, respectively. The entropy S is given as follows:

$$S = -\sum_{\vec{p},\eta,\tau,\alpha} \left\{ n_{\vec{p}}^{(\eta)} \log n_{\vec{p}}^{(\eta)} + \left(1 - n_{\vec{p}}^{(\eta)}\right) \log \left(1 - n_{\vec{p}}^{(\eta)}\right) + \bar{n}_{\vec{p}}^{(\eta)} \log \bar{n}_{\vec{p}}^{(\eta)} + \left(1 - \bar{n}_{\vec{p}}^{(\eta)}\right) \log \left(1 - \bar{n}_{\vec{p}}^{(\eta)}\right) \right\}.$$

Using the following identities:

$$n_{\vec{p}}^{(\eta)} \log n_{\vec{p}}^{(\eta)} = -n_{\vec{p}}^{(\eta)} \times \frac{E_{\vec{p}}^{(\eta)} - \mu}{T} - n_{\vec{p}}^{(\eta)} \log \left(1 - n_{\vec{p}}^{(\eta)}\right),$$

$$\bar{n}_{\vec{p}}^{(\eta)} \log \bar{n}_{\vec{p}}^{(\eta)} = -\bar{n}_{\vec{p}}^{(\eta)} \times \frac{E_{\vec{p}}^{(\eta)} + \mu}{T} - \bar{n}_{\vec{p}}^{(\eta)} \log \left(1 - \bar{n}_{\vec{p}}^{(\eta)}\right),$$

the above Ω can be recast into

$$\Omega = -\sum_{\vec{p},\eta,\tau,\alpha} \left\{ E_{\vec{p}}^{(\eta)} + T \log \left(1 + \exp\left(-\frac{E_{\vec{p}}^{(\eta)} - \mu}{T}\right)\right) + T \log \left(1 + \exp\left(-\frac{E_{\vec{p}}^{(\eta)} + \mu}{T}\right)\right) \right\} + \frac{M^2}{4G_S} + \frac{F^2}{2G_T}.$$

Let us change the summation over momenta into integration, and then let us introduce polar coordinates, $p_1 = p_T \cos\theta$, $p_2 = p_T \sin\theta$, so as to integrate. The domain of integration is obtained as follows:

$$-\sqrt{\Lambda^2 - p_T^2} \le p_3 \le \sqrt{\Lambda^2 - p_T^2}, \quad 0 \le p_T \le \Lambda.$$

After integrating over θ and summing over τ and α, we get the final form:

$$\Omega(M, F, \mu, T) = -\frac{3}{\pi^2} \sum_{\eta} \int_0^{\Lambda} dp_T \int_0^{\sqrt{\Lambda^2 - p_T^2}} dp_3 \, p_T \times \left\{ E_{\vec{p}}^{(\eta)} + T \log \left(1 + \exp\left(-\frac{E_{\vec{p}}^{(\eta)} - \mu}{T}\right)\right) + T \log \left(1 + \exp\left(-\frac{E_{\vec{p}}^{(\eta)} + \mu}{T}\right)\right) \right\} + \frac{M^2}{4G_S} + \frac{F^2}{2G_T}. \tag{4.2}$$

5. Numerical results and discussions

In this section we would like to discuss the thermodynamic potential at zero/finite temperature numerically. In order to evaluate it we use the three-momentum cutoff parameter and coupling constants in Table 1. Here, we adopt the strength of the tensor interaction G_T as a rather small value compared with the one used in our previous paper. The reason why we take G_T as a rather small value, 11.0 GeV, is that the vacuum polarization, namely, the contribution of the negative energy sea, is taken into account. A detailed discussion of this effect has already been given in Appendix B in Ref. [15]. Here, in this section, we show numerical results in the case of the chiral limit, $m_0 = 0.0$.

Table 1. Parameter set.

Λ/GeV	m_0/GeV	G_S/GeV^{-2}	G_T/GeV^{-2}
0.631	0.0	5.5	11.0

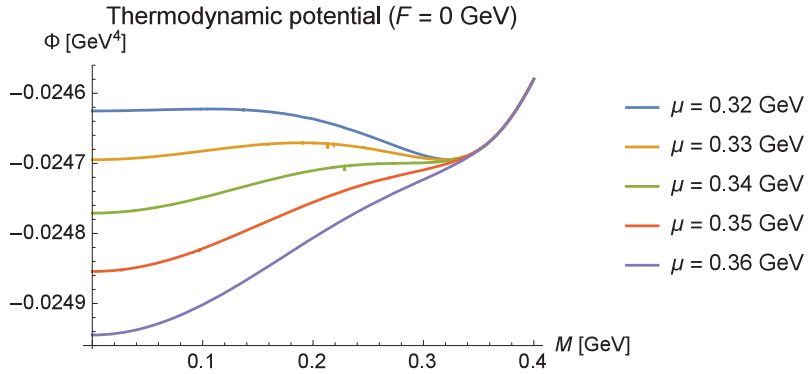

Fig. 1. The thermodynamic potential with $F = 0$ is depicted as a function of the constituent quark mass M in various quark chemical potentials.

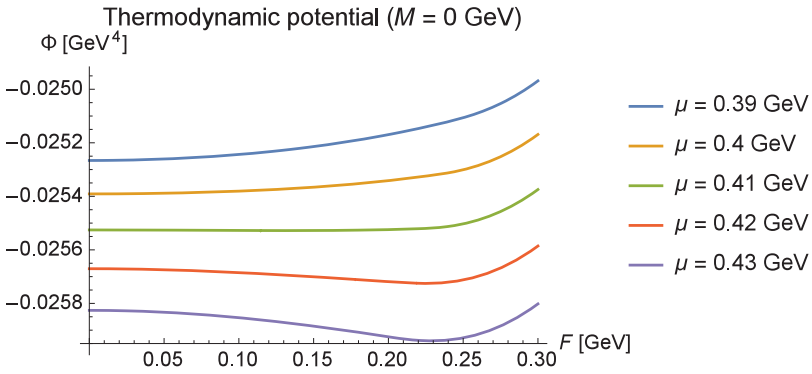

Fig. 2. The thermodynamic potential with $M = 0$ is depicted as a function of the spin-polarized condensate F in various quark chemical potentials.

5.1. Thermodynamic potential at zero temperature

Let us discuss the thermodynamic potential at zero temperature. First we consider the chiral condensate M and the spin polarization F separately.

Figure 1 shows the thermodynamic potential in the special case where $F = 0$. When the chemical potential has a value below 0.32 GeV and above 0.35 GeV, the thermodynamic potential has only one minimum. On the other hand, when $\mu = 0.33 \sim 0.34$ GeV, the thermodynamic potential has two local minima. This indicates that the phase transition to chiral condensate is of first order.

Figure 2 shows the thermodynamic potential for $M = 0$. When the chemical potential is small, the spin-polarized phase does not appear. However, when the chemical potential μ has a value above 0.42 GeV, the spin-polarized phase appears. This figure shows that the phase transition to spin polarization is of second order.

Next, let us consider M and F simultaneously. In Fig. 3, the contour map for the thermodynamic potential is depicted with various quark chemical potentials. The horizontal and vertical axes

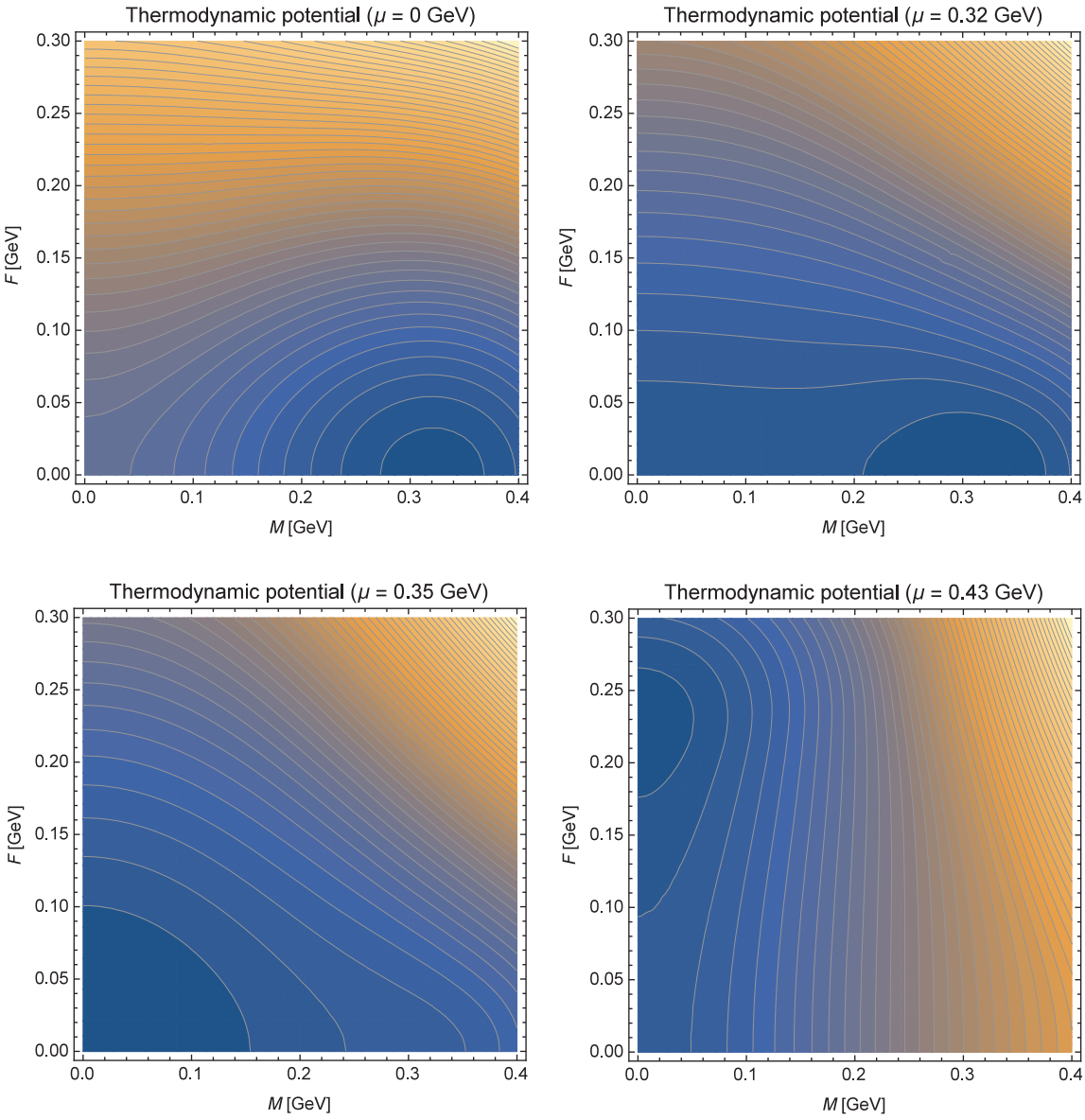

Fig. 3. The contour map of the thermodynamic potential is depicted as a function of the constituent quark mass M and the spin-polarized condensate F in various quark chemical potentials. The horizontal and vertical axes represent M and F, respectively. Darker colors represent a lower thermodynamic potential.

represent the constituent quark mass M and the spin-polarized condensate F, respectively. When μ varies from 0 GeV to 0.32 GeV, the chiral-condensed phase arises. However, when μ reaches 0.35 GeV, chiral symmetry is restored. If $\mu = 0.43$ GeV, the spin-polarized phase appears. These contour maps indicate that the two phases, the chiral-condensed and spin-polarized phases, do not coexist.

Here, two points should be mentioned. One is about the effect of G_T, namely, the coupling strength of the tensor-type interaction. As has already been mentioned at the beginning of this section, a detailed discussion about G_T has already been given in Appendix B in Ref. [15]. However, let us demonstrate the effect of G_T for the spin polarization. Figure 4 shows the thermodynamic potential with $M = 0$ at various values of G_T, namely, $G_T/G_S = 1, 5, 2.0$, and 2.5, respectively. As the coupling strength G_T is increased, the critical chemical potential of the phase transition decreases.

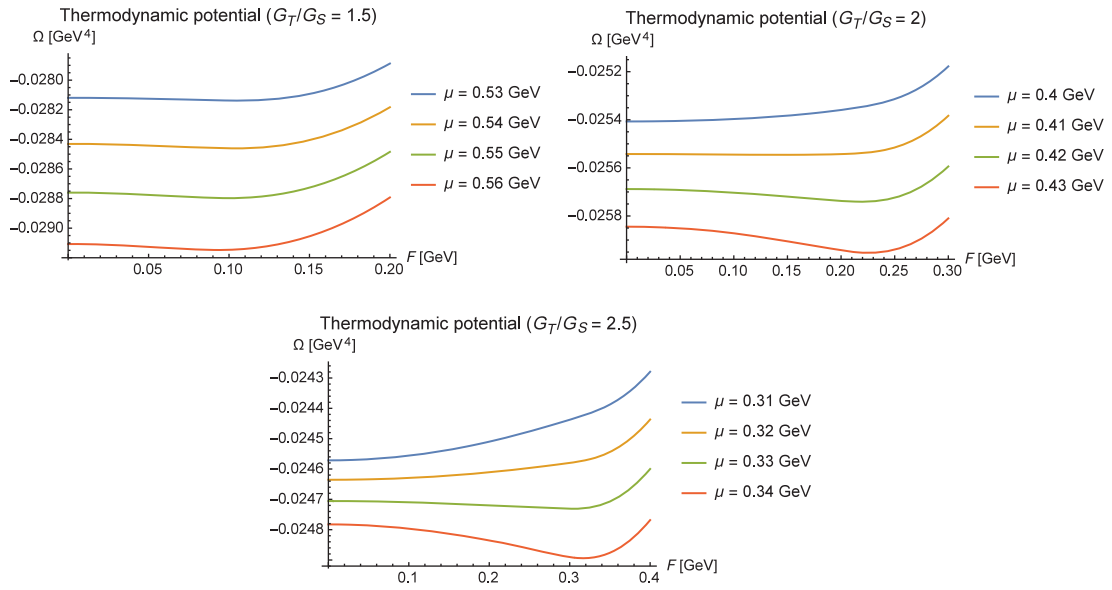

Fig. 4. The thermodynamic potentials with $M = 0$ and $T = 0.01$ are depicted at various ratios of G_T/G_S. The ratios $G_T/G_S = 1.5$, 2, and 2.5 mean $G_T = 8.25$, 11.0, and 3.75 GeV^{-2}, respectively.

For example, at small values of G_T such as $G_T/G_S = 1.5$, the phase transition occurs around $\mu = 0.54$ GeV. On the other hand, at large G_T, $G_T/G_S = 2.5$, the phase transition occurs around $\mu = 0.33$ GeV. In this paper, we adopt a moderate value $G_T/G_S = 2.0$ for discussions.

Secondly, we mention the reason why the spin polarization occurs at large chemical potential. At zero temperature, the spin-polarized phase is actually realized in our model. It is easy to understand how the spin-polarized phase appears. Neglecting the contribution of the chiral condensate, the energy E of the system under consideration can be expressed by using the quark chemical potential as

$$\begin{aligned} E &= \int^{\mu} \mu \frac{\partial N}{\partial \mu} d\mu + \frac{F^2}{2G_T} \\ &= \mu N - \int N \, d\mu + \frac{F^2}{2G_T}. \end{aligned} \tag{5.1}$$

Thus, the thermodynamical potential $\Phi (= E - \mu N)$ is obtained as

$$\begin{aligned} \Phi &= E - \mu N \\ &= -\int N \, d\mu + \frac{F^2}{2G_T} \\ &= -\int d\mu \sum_{\eta,\tau,\alpha} \int \frac{d^3\boldsymbol{p}}{(2\pi)^3} \theta\left(\mu - E_{\vec{p}}^{(\eta)}\right) + \frac{F^2}{2G_T}, \end{aligned} \tag{5.2}$$

where $\theta(x)$ represents the Heaviside step function. Let us consider the normal quark matter in which $F = 0$. In this case, the above-derived thermodynamical potential can be calculated easily as

$$\Phi = -\frac{\mu^4}{2\pi^2}. \tag{5.3}$$

On the other hand, in the case $F \neq 0$, we can also calculate the thermodynamic potential analytically; this was presented in Ref. [20]. For simplicity, let us consider the case $F > \mu$. For $F > \mu$, $E_{\vec{p}}^{(+)}$ does

not contribute to the three-momentum integration. In this case, by the existence of the theta function, the integration has a finite value in $E_{\vec{p}}^{(-)} \leq \mu$:

$$E_{\vec{p}}^{(-)} \equiv \sqrt{p_3^2 + \left(F - \sqrt{p_1^2 + p_2^2}\right)^2} \leq \mu. \tag{5.4}$$

The equality in the above expression represents the formula of a torus in which the major radius is F and the small radius is μ. Thus, the Fermi surface has the form of a torus. Therefore, the momentum integral $\int d^3\mathbf{p}\theta\left(\mu - E_{\vec{p}}^{(-)}\right)$ means the volume of the Fermi "torus", where the volume gives $2\pi^2\mu^2 F$ $\left(=\pi\mu^2 \cdot 2\pi F\right)$. Then, we obtain the thermodynamical potential in the large-μ region as

$$\begin{aligned}\Phi &= -\frac{3}{4\pi^3}\int^{\mu} d\mu 2\pi^2\mu^2 F + \frac{F^2}{2G_T} \\ &= -\frac{\mu^3 F}{2\pi} + \frac{F^2}{2G_T}.\end{aligned} \tag{5.5}$$

The "gap equation" for F is derived from

$$\frac{\partial\Phi}{\partial F} = -\frac{\mu^3}{2\pi} + \frac{F}{G_T} = 0, \quad \text{thus,} \quad F = \frac{G_T\mu^3}{2\pi}. \tag{5.6}$$

Inserting the above-derived F into the thermodynamical potential, we finally obtain

$$\Phi = -\frac{G_T\mu^6}{8\pi^2}. \tag{5.7}$$

For small chemical potential, namely, at low quark number density, normal quark matter is realized because the thermodynamic potential has order μ^4. On the other hand, for large chemical potential, namely, at high quark number density, the thermodynamical potential with the order of μ^6 overcomes the normal quark matter with the order of μ^4. It may be concluded that the appearance of the spin-polarized phase is due to the effect of the volume of the phase space. Thus, at high density, the spin-polarized phase is realized absolutely.

5.2. Thermodynamic potential at finite temperature

Let us consider the thermodynamic potential at finite temperature. First, let us treat the two cases without M or F separately. Figure 5 shows the thermodynamic potential at finite temperature for $F = 0$. If the temperature T is not so high, the chiral-condensed phase is realized. However, in the high-temperature region, the chiral-condensed phase disappears. It should be noted that, in the cases with $\mu = 0\,\text{GeV}$ and $\mu = 0.2\,\text{GeV}$, the phase transition is of second order, while the phase transition is of first order in the case $\mu = 0.32\,\text{GeV}$.

Secondly, we discuss the case for $M = 0$. In Fig. 6, it is shown that the spin-polarized phase is realized in the low-temperature region only. If temperature rises, the spin polarization disappears rapidly. In this case, the phase transition from the spin-polarized phase to the normal phase is of second order.

Finally, let us consider M and F simultaneously. It is shown in Fig. 7 that chiral symmetry is broken for small chemical potential and low temperature. However, if the chemical potential or temperature becomes high, chiral symmetry is restored. In the large chemical potential and low-temperature region, the spin-polarized condensate appears. However, for higher temperatures, it disappears. According to these contour maps, it may be concluded that the two phases, namely, the chiral-condensed phase and the spin-polarized phase, do not coexist at finite temperature.

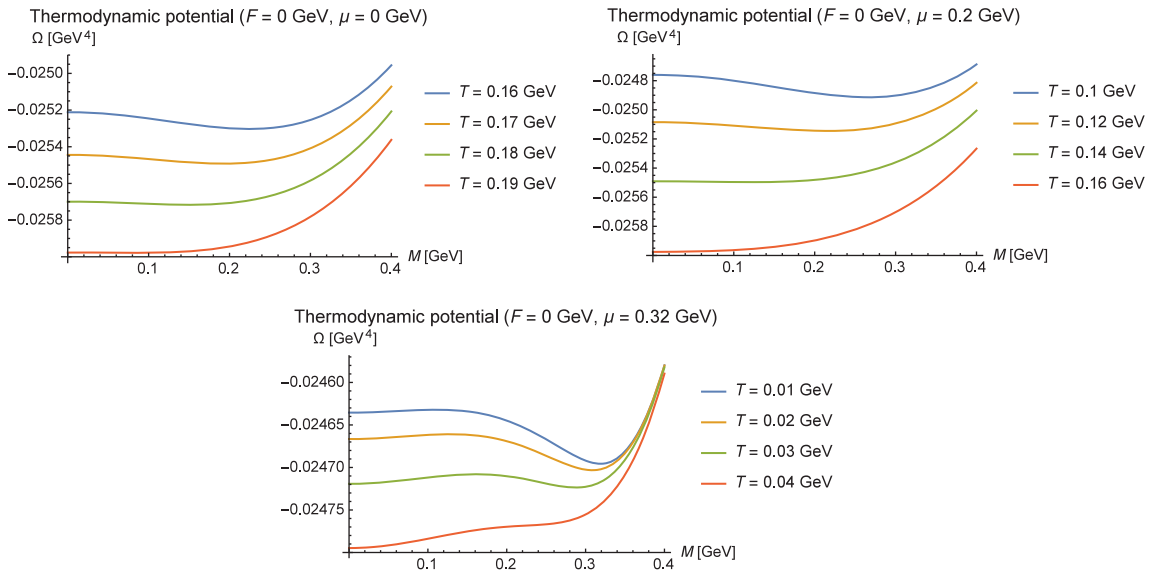

Fig. 5. The thermodynamic potentials with $F = 0$ are depicted at various temperatures T with the chemical potential $\mu = 0\,\text{GeV}$, $0.2\,\text{GeV}$, and $0.32\,\text{GeV}$, respectively. The horizontal and vertical axes represent the constituent quark mass M and the thermodynamic potential $\Omega(M, \mu, T)$, respectively.

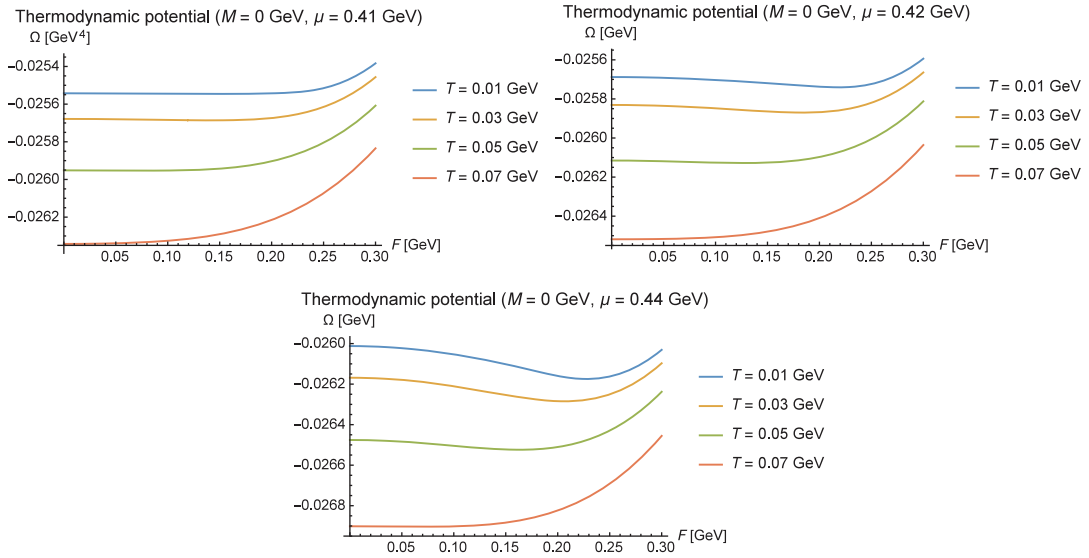

Fig. 6. The thermodynamic potentials with $M = 0$ are depicted at various temperatures T with the chemical potential $\mu = 0.41\,\text{GeV}$, $0.42\,\text{GeV}$, and $0.44\,\text{GeV}$, respectively. The horizontal and vertical axes represent the spin-polarized condensate F and the thermodynamic potential $\Omega(F, \mu, T)$, respectively.

5.3. Phase diagram on the T–μ plane

In summary, it is possible to show the regions of the chiral-condensed phase and the spin-polarized phase on a plane with temperature T and quark chemical potential μ and also to draw the phase boundary indicating the order of phase transition under the chiral limit, $m_0 = 0$. In Fig. 8, the phase diagram in this model is presented. As is shown in this phase diagram, the chiral-condensed phase exists on the left-hand side of the T–μ plane and the spin-polarized phase exists on the right. It is indicated that, for the boundary of the chiral-condensed and normal phases, there is a critical end-point for the phase transition near $\mu = 0.31\,\text{GeV}$ and $T = 0.046\,\text{GeV}$. On the other hand, the phase

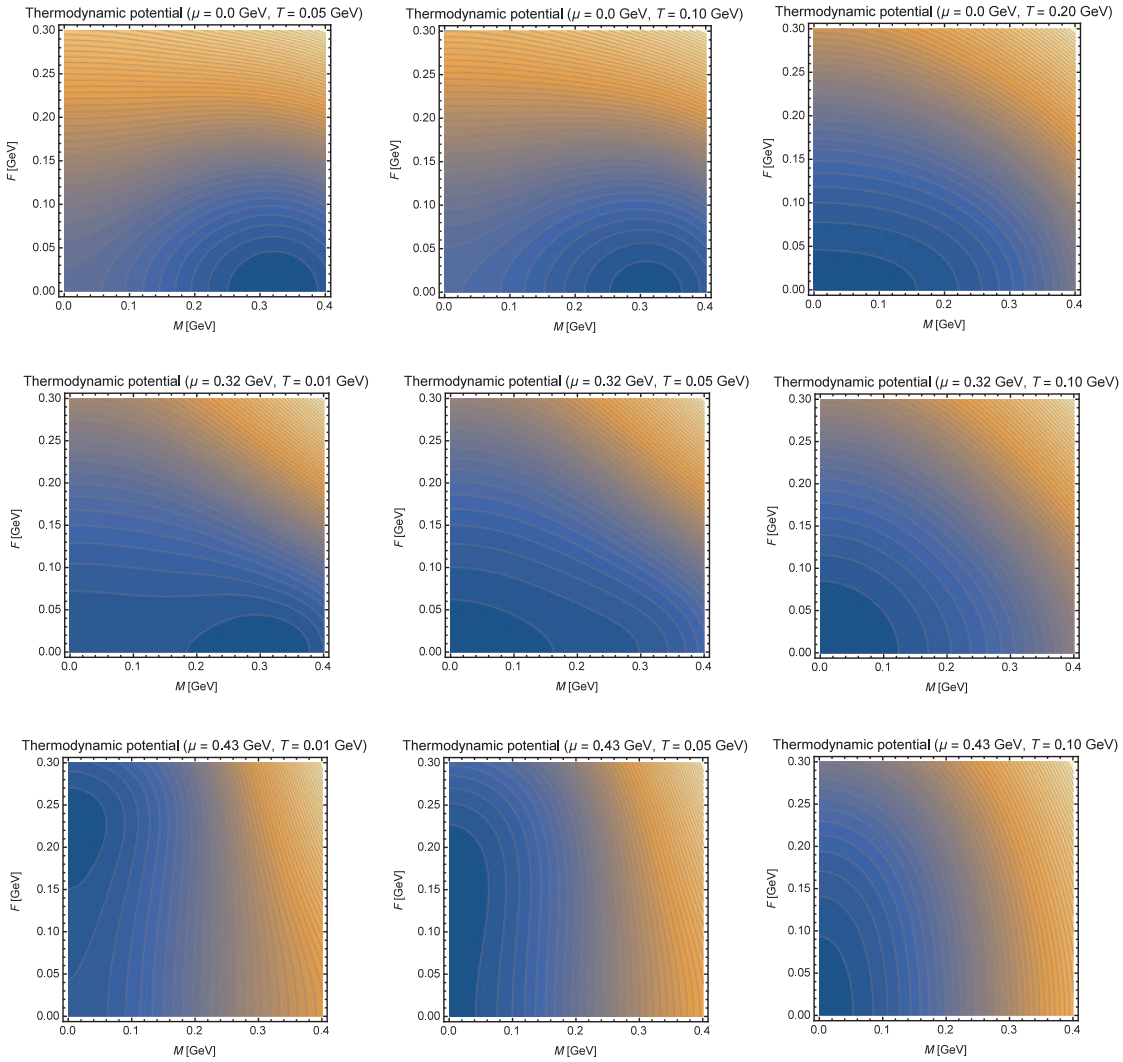

Fig. 7. The contour maps of the thermodynamic potential are depicted as a function of the constituent quark mass M and the spin-polarized condensate F at various quark chemical potentials and temperatures. The horizontal and vertical axes represent M and F, respectively.

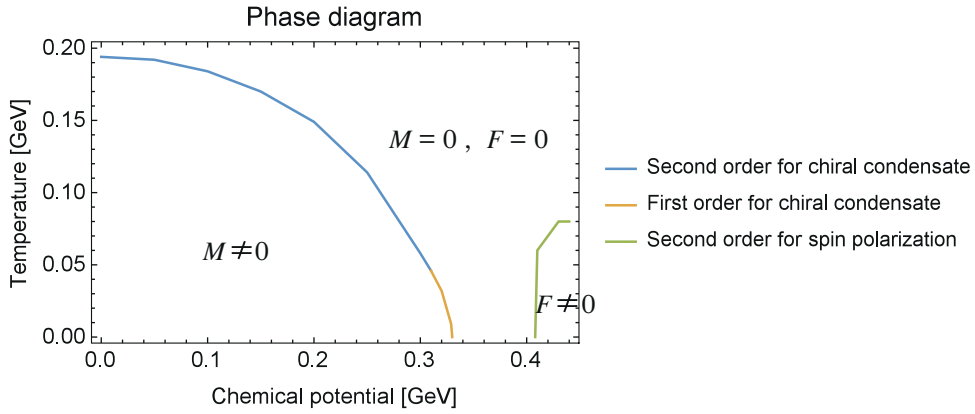

Fig. 8. The phase diagram in our model. The horizontal and vertical axes represent the quark chemical potential and the temperature, respectively.

transition from the normal quark phase to the spin-polarized phase is always of second order and there is no endpoint.

6. Summary and concluding remarks

In this paper, it has been shown that the spin-polarized phase appears in the region with a large quark chemical potential and low temperature by using the NJL model with tensor-type four-point interaction between quarks. We have considered the chiral condensate and spin-polarized condensate simultaneously. For rather low density, the chiral condensate exists and spin-polarized condensate does not exist. As the quark chemical potential is increased, the chiral condensate disappears and the spin-polarized condensate arises. Thus, the spin-polarized phase may exist in the high-density and low-temperature region in the QCD phase diagram. However, it may be concluded that the two phases do not coexist in this model under the parameter set adopted here.

It should also be indicated that the color superconducting phase may be realized in the region with high density and low temperature. However, at zero temperature, the spin-polarized phase may be realized instead of the two-flavor color superconducting phase in the case with only two flavors [9]. It would be interesting to see whether the spin-polarized phase survives at finite temperature instead of the color superconducting phase. It is one of future important problems to investigate. Furthermore, in this paper, we do not consider the electromagnetic field at all. It is also important to study the electromagnetic properties of the spin-polarized phase, e.g., spontaneous magnetization in compact stars. In particular, the charge neutrality and β-equilibrium would play an essential role in a discussion of the physics of neutron stars and/or magnetars. This is also an interesting future problem.

Acknowledgements

One of the authors (Y.T.) is partially supported by Grants-in-Aid of the Scientific Research (No. 26400277) from the Ministry of Education, Culture, Sports, Science and Technology in Japan.

Funding

Open Access funding: SCOAP[3].

Appendix A. Derivation of the thermodynamic potential at zero temperature from that at finite temperature

In this appendix we derive the thermodynamic potential at zero temperature from that at finite temperature. The thermodynamic potential at finite temperature is as follows:

$$\Omega(M, F, \mu, T) = -\sum_{\eta,\tau,\alpha} \int_{\vec{p}^2 \le \Lambda^2} \frac{d^3p}{(2\pi)^3} \left\{ E_{\vec{p}}^{(\eta)} + T \log\left(1 + \exp\left(-\frac{E_{\vec{p}}^{(\eta)} - \mu}{T}\right)\right) + T \log\left(1 + \exp\left(-\frac{E_{\vec{p}}^{(\eta)} + \mu}{T}\right)\right)\right\} + \frac{F^2}{2G_T} + \frac{M^2}{4G_S}. \tag{A1}$$

If we assume that $T \ll 1$, we can carry out the Taylor expansion for the logarithmic function in the following way:

$$T \log\left(1+\exp\left(-\frac{E_{\vec{p}}^{(\eta)}-\mu}{T}\right)\right) \to \begin{cases} -\left(E_{\vec{p}}^{(\eta)}-\mu\right)+T\exp\left(\dfrac{E_{\vec{p}}^{(\eta)}-\mu}{T}\right) & \text{for } E_{\vec{p}}^{(\eta)} \le \mu \\ T\exp\left(-\dfrac{E_{\vec{p}}^{(\eta)}-\mu}{T}\right) & \text{for } E_{\vec{p}}^{(\eta)} > \mu, \end{cases}$$

$$T \log\left(1+\exp\left(-\frac{E_{\vec{p}}^{(\eta)}+\mu}{T}\right)\right) \to T\exp\left(-\frac{E_{\vec{p}}^{(\eta)}+\mu}{T}\right). \tag{A2}$$

Furthermore, in the region where $T \to 0$, we can reduce the above expressions to

$$T \log\left(1+\exp\left(-\frac{E_{\vec{p}}^{(\eta)}-\mu}{T}\right)\right) \to -\left(E_{\vec{p}}^{(\eta)}-\mu\right)\theta\left(\mu-E_{\vec{p}}^{(\eta)}\right),$$

$$T \log\left(1+\exp\left(-\frac{E_{\vec{p}}^{(\eta)}+\mu}{T}\right)\right) \to 0, \tag{A3}$$

where $\theta(x)$ is the step function. Using these results, we can rewrite $\Omega(M, F, \mu, T)$ as

$$\Omega(M,F,\mu,T) \to -\sum_{\eta,\tau,\alpha}\int_{\vec{p}^2\le\Lambda^2}\frac{d^3p}{(2\pi)^3}\left\{E_{\vec{p}}^{(\eta)}-\left(E_{\vec{p}}^{(\eta)}-\mu\right)\theta\left(\mu-E_{\vec{p}}^{(\eta)}\right)\right\} + \frac{F^2}{2G_T}+\frac{M^2}{4G_S}. \tag{A4}$$

This expression is simply that of the thermodynamic potential at zero temperature.

Appendix B. Derivation of the effective potential with the functional method

Let us start with the following Lagrangian density in order to derive the effective potential by using the functional method:

$$\begin{aligned}\mathcal{L} &= \bar{\psi}\left(i\gamma^\mu\partial_\mu - m_0\right)\psi + G_S\left(\bar{\psi}\psi\right)^2 - \frac{G_T}{2}\left(\bar{\psi}\gamma^1\gamma^2\tau_3\psi\right)\left(\bar{\psi}\gamma_1\gamma_2\tau_3\psi\right) \\ &= \bar{\psi}\left(i\gamma^\mu\partial_\mu - m_0\right)\psi + G_S\left(\bar{\psi}\psi\right)^2 + \frac{G_T}{2}\left(\bar{\psi}\Sigma_3\psi\right)^2, \end{aligned} \tag{B1}$$

where we define $\Sigma_3 \equiv -i\gamma^1\gamma^2$. In order to perform the functional integration, let us introduce two auxiliary fields, M' and F, and use the following unit relation:

$$\begin{aligned}1 = \int \mathcal{D}M'\mathcal{D}F \exp\left[-i\int d^4x\left\{M'+G_S\left(\bar{\psi}\psi\right)\right\}G_S^{-1}\left\{M'+G_S\left(\bar{\psi}\psi\right)\right\}\right] \\ \times \exp\left[-\frac{i}{2}\int d^4x\left\{F+G_T\left(\bar{\psi}\Sigma_3\psi\right)\right\}G_T^{-1}\left\{F+G_T\left(\bar{\psi}\Sigma_3\psi\right)\right\}\right]. \end{aligned} \tag{B2}$$

The generating functional Z for the Lagrangian density (B1) is given as follows:

$$Z \propto \int \mathcal{D}\bar{\psi}\mathcal{D}\psi \exp\left[i\int d^4x\left\{\bar{\psi}\left(i\gamma^\mu\partial_\mu - m_0\right)\psi + G_S\left(\bar{\psi}\psi\right)^2 + \frac{G_T}{2}\left(\bar{\psi}\Sigma_3\psi\right)^2\right\}\right]. \tag{B3}$$

Inserting the unit relation (B2) into Z and setting $M' = M/2$, we obtain

$$Z \propto \int \mathcal{D}\bar{\psi}\ \mathcal{D}\psi\ \mathcal{D}M\ \mathcal{D}F \exp\left[i \int d^4x \left\{ \bar{\psi}\left(i\gamma^\mu \partial_\mu - M_q - F\Sigma_3 \right)\psi - \frac{M^2}{4G_S} - \frac{F^2}{2G_T} \right\} \right], \quad \text{(B4)}$$

where we define $M_q \equiv m_0 + M$. Thus, we can integrate out with respect to ψ and $\bar{\psi}$ easily. After some calculations, we get

$$\begin{aligned} Z &\propto \int \mathcal{D}M\ \mathcal{D}F\ \mathrm{Det}\left(i\gamma^\mu \partial_\mu - M_q - F\Sigma_3 \right) \exp\left[-i \int d^4x \left(\frac{M^2}{4G_S} + \frac{F^2}{2G_T} \right) \right] \\ &= \int \mathcal{D}M\ \mathcal{D}F \exp\left[\mathrm{Tr}\log\det\left(i\gamma^\mu \partial_\mu - M_q - F\Sigma_3 \right) - i \int d^4x \left(\frac{M^2}{4G_S} + \frac{F^2}{2G_T} \right) \right], \end{aligned} \quad \text{(B5)}$$

where, in the second line, the determinant, det, operates on gamma matrices. In order to compute the trace, Tr, we change to momentum space:

$$\begin{aligned} Z \propto \int \mathcal{D}M\ \mathcal{D}F \exp\left[i N_C N_F \int d^4x \frac{d^4p}{i\,(2\pi)^4} \log\det\left(\not{p} - M_q - F\Sigma_3 \right) \right] \\ \times \exp\left[-i \int d^4x \left(\frac{M^2}{4G_S} + \frac{F^2}{2G_T} \right) \right], \end{aligned} \quad \text{(B6)}$$

where N_C and N_F mean the color and flavor numbers, respectively. Our next step is to calculate the determinant. We can do this as follows:

$$\begin{aligned} \det\left(\not{p} - M_q - F\Sigma_3 \right) &= \det\gamma^0 \left(\not{p} - M_q - F\Sigma_3 \right) \\ &= \det\left[p^0 - \gamma^0 \left(\vec{\gamma}\cdot\vec{p} + M_q + F\Sigma_3 \right) \right] \\ &= \det\left[p^0 - \begin{pmatrix} E_{\vec{p}}^{(+)} & & & \\ & E_{\vec{p}}^{(-)} & & \\ & & -E_{\vec{p}}^{(+)} & \\ & & & -E_{\vec{p}}^{(-)} \end{pmatrix} \right] \\ &= \left(p^0 - E_{\vec{p}}^{(+)} \right)\left(p^0 - E_{\vec{p}}^{(-)} \right)\left(p^0 + E_{\vec{p}}^{(+)} \right)\left(p^0 + E_{\vec{p}}^{(-)} \right). \end{aligned} \quad \text{(B7)}$$

Substituting the above result into Z in (B6), we obtain

$$\begin{aligned} Z \propto \int \mathcal{D}M\ \mathcal{D}F \\ \times \exp\left[i N_C N_F \int d^4x \frac{d^4p}{i\,(2\pi)^4} \log\left(p^0 - E_{\vec{p}}^{(+)} \right)\left(p^0 - E_{\vec{p}}^{(-)} \right)\left(p^0 + E_{\vec{p}}^{(+)} \right)\left(p^0 + E_{\vec{p}}^{(-)} \right) \right] \\ \times \exp\left[-i \int d^4x \left(\frac{M^2}{4G_S} + \frac{F^2}{2G_T} \right) \right]. \end{aligned} \quad \text{(B8)}$$

To start with, we consider only the contents of the exponential in the second line in (B8):

$$\int \frac{d^4p}{i\,(2\pi)^4} \log\left(p^0 - E_{\vec{p}}^{(+)} \right)\left(p^0 - E_{\vec{p}}^{(-)} \right)\left(p^0 + E_{\vec{p}}^{(+)} \right)\left(p^0 + E_{\vec{p}}^{(-)} \right). \quad \text{(B9)}$$

Let us differentiate and integrate the above expression with respect to $E_{\vec{p}}^{(+)}$ and $E_{\vec{p}}^{(-)}$. As a result, (B9) can be recast into

$$\int \frac{d^4p}{i\,(2\pi)^4} \int dE_{\vec{p}}^{(+)} \left(\frac{1}{p^0 + E_{\vec{p}}^{(+)}} - \frac{1}{p^0 - E_{\vec{p}}^{(+)}} \right) + \int \frac{d^4p}{i\,(2\pi)^4} \int dE_{\vec{p}}^{(-)} \left(\frac{1}{p^0 + E_{\vec{p}}^{(-)}} - \frac{1}{p^0 - E_{\vec{p}}^{(-)}} \right). \tag{B10}$$

We would like to discuss a system at finite temperature and density. So let us change the integration to a summation by using the Matsubara method as follows:

$$\int \frac{d^4p}{i\,(2\pi)^4} f\left(p^0, \vec{p}\right) \to T \sum_{n=-\infty}^{\infty} \int \frac{d^3p}{(2\pi)^3} f\left(i\omega_n + \mu, \vec{p}\right), \tag{B11}$$

where ω_n is the Matsubara frequency and μ is the chemical potential. Using the formula

$$\lim_{\epsilon \to +0} T \sum_n \frac{e^{i\omega_n \epsilon}}{i\omega_n - x} = \lim_{\epsilon \to +0} \frac{e^{i\omega_n \epsilon}}{e^{x/T} + 1} = \frac{1}{e^{x/T} + 1}, \tag{B12}$$

we can calculate the summation following the standard technique. As a result, we obtain

$$\sum_{\eta=\pm} \int \frac{d^3p}{(2\pi)^3} \left[E_{\vec{p}}^{(\eta)} + \mu + T \log \left\{ 1 + \exp\left(-\frac{E_{\vec{p}}^{(\eta)} + \mu}{T} \right) \right\} + T \log \left\{ 1 + \exp\left(-\frac{E_{\vec{p}}^{(\eta)} - \mu}{T} \right) \right\} \right]. \tag{B13}$$

Substituting the above result into Z, Z can be expressed as

$$Z \propto \int \mathcal{D}M \mathcal{D}F \exp i \left[N_C N_F \int d^4x \frac{d^3p}{(2\pi)^3} \sum_\eta \left(E_{\vec{p}}^{(\eta)} + T \log \left\{ 1 + \exp\left(-\frac{E_{\vec{p}}^{(\eta)} + \mu}{T} \right) \right\} + T \log \left\{ 1 + \exp\left(-\frac{E_{\vec{p}}^{(\eta)} - \mu}{T} \right) \right\} \right) - \int d^4x \left(\frac{M^2}{4G_S} + \frac{F^2}{2G_T} \right) \right], \tag{B14}$$

where we neglect a constant term. In general, the effective action Γ and effective potential V are defined as follows:

$$Z = \exp(i\Gamma[M, F, T, \mu]), \quad V[M, F, T, \mu] = -\frac{\Gamma[M, F, T, \mu]}{\int d^4x}. \tag{B15}$$

Thus, finally, we obtain the effective potential V as

$$V[M, F, T, \mu] = -N_C N_F \int \frac{d^3p}{(2\pi)^3} \sum_\eta \left[E_{\vec{p}}^{(\eta)} + T \log \left\{ 1 + \exp\left(-\frac{E_{\vec{p}}^{(\eta)} + \mu}{T} \right) \right\} + T \log \left\{ 1 + \exp\left(-\frac{E_{\vec{p}}^{(\eta)} - \mu}{T} \right) \right\} \right] + \frac{M^2}{4G_S} + \frac{F^2}{2G_T}. \tag{B16}$$

This is identical with the thermodynamic potential (4.2).

Appendix C. The domain of integration with respect to the three-momentum in the thermodynamic potential at zero temperature

In Sect. 3, we gave the expression of the thermodynamic potential. In this appendix, we give a domain of integration with respect to the three-momentum. We assume that $M \geq 0$, $F \geq 0$, and $\Lambda > \mu$ without loss of generality and introduce polar coordinates (p_T, θ):

$$p_1 = p_T \cos\theta, \quad p_2 = p_T \sin\theta.$$

Moreover, we define $q \equiv \sqrt{p_T^2 + M_{\rm q}^2}$ in order to integrate over momenta. After integrating over θ in Eqs. (3.4)–(3.6), we obtain the thermodynamic potential $\Phi = \sum_{i=1}^{4} \Phi_i$ as follows:

$$\begin{aligned}
\Phi_1(M, F, \mu) &= \frac{3}{2\pi^2} \int_{\Gamma_1} dq\, dp_3\, q \left(\sqrt{p_3^2 + (q+F)^2} - \mu \right), \\
\Gamma_1 &= \left\{ p_3^2 + (q+F)^2 \leq \mu^2,\, p_3^2 + q^2 \leq \Lambda^2 + M_{\rm q}^2,\, q \geq M_{\rm q} \right\} \\
\Phi_2(M, F, \mu) &= \frac{3}{2\pi^2} \int_{\Gamma_2} dq\, dp_3\, q \left(\sqrt{p_3^2 + (q-F)^2} - \mu \right), \\
\Gamma_2 &= \left\{ p_3^2 + (q-F)^2 \leq \mu^2,\, p_3^2 + q^2 \leq \Lambda^2 + M_{\rm q}^2,\, q \geq M_{\rm q} \right\} \\
\Phi_3(M, F, \mu) &= -\frac{3}{2\pi^2} \sum_{\eta} \int_{\Gamma_3} dq\, dp_3\, q \sqrt{p_3^2 + (q + \eta F)^2}, \\
\Gamma_3 &= \left\{ p_3^2 + q^2 \leq \Lambda^2 + M_{\rm q}^2,\, q \geq M_{\rm q} \right\} \\
\Phi_4(M, F, \mu) &= \frac{M^2}{4G_S} + \frac{F^2}{2G_T}.
\end{aligned}$$

Further, let us integrate the thermodynamic potential over p_3 analytically. To do this we must discuss the domain of integration carefully. First we consider Φ_1 and Γ_1. If the first condition in Γ_1 is satisfied, the second condition in it will be satisfied automatically. So we can reduce Γ_1 to

$$\Gamma_1 = \left\{ p_3^2 + (q+F)^2 \leq \mu^2, q \geq M_{\rm q} \right\}.$$

Furthermore, we can change the above condition to the following:

$$\Gamma_1 = \left\{ -\sqrt{\mu^2 - (q+F)^2} \leq p_3 \leq \sqrt{\mu^2 - (q+F)^2}, q \geq M_{\rm q} \right\}.$$

Since the contents of the square root must be positive, the final form is

$$\Gamma_1 = \left\{ -\sqrt{\mu^2 - (q+F)^2} \leq p_3 \leq \sqrt{\mu^2 - (q+F)^2}, M_{\rm q} \leq q \leq \mu - F \right\}.$$

However, we need the condition $M_{\rm q} \leq \mu - F$ in order to integrate over q. If $M_{\rm q} > \mu - F$, we cannot perform the integration. Using an integration formula,

$$\int dx\, \sqrt{x^2 + a^2} = \tfrac{1}{2} \left\{ x\sqrt{x^2 + a^2} + a^2 \log\left(x + \sqrt{x^2 + a^2} \right) \right\},$$

we were able to perform the integration over p_3 easily. The final results are as follows:

If $M_{\rm q} > \mu - F$,

$$\Phi_1(M, F, \mu) = 0. \tag{C1a}$$

If $M_{\rm q} \leq \mu - F$,

$$\Phi_1(M, F, \mu) = \frac{3}{2\pi^2} \int_{M_{\rm q}}^{\mu - F} dq\, q \left\{ -\mu \sqrt{\mu^2 - (q+F)^2} + (q+F)^2 \log \left(\frac{\sqrt{\mu^2 - (q+F)^2} + \mu}{q+F} \right) \right\}. \quad \text{(C1b)}$$

Next, we consider Φ_2 and Γ_2. This case is more complicated than the previous case. There are five cases for conditions to perform the integration, as follows:

If $F - \mu \leq M_{\rm q} \leq F + \mu \leq \sqrt{\Lambda^2 + M_{\rm q}^2}$,

$$\Phi_2(M, F, \mu) = \frac{3}{2\pi^2} \int_{M_{\rm q}}^{F+\mu} dq \int_{-\sqrt{\mu^2-(q-F)^2}}^{\sqrt{\mu^2-(q-F)^2}} dp_3\, q \left(\sqrt{p_3^2 + (q-F)^2} - \mu \right).$$

If $M_{\rm q} \leq F - \mu \leq F + \mu \leq \sqrt{\Lambda^2 + M_{\rm q}^2}$,

$$\Phi_2(M, F, \mu) = \frac{3}{2\pi^2} \int_{F-\mu}^{F+\mu} dq \int_{-\sqrt{\mu^2-(q-F)^2}}^{\sqrt{\mu^2-(q-F)^2}} dp_3\, q \left(\sqrt{p_3^2 + (q-F)^2} - \mu \right).$$

If $M_{\rm q} \leq F - \mu \leq b \leq \sqrt{\Lambda^2 + M_{\rm q}^2} \leq F + \mu$,

$$\Phi_2(M, F, \mu) = \frac{3}{2\pi^2} \left(\int_{F-\mu}^{b} \int_{-\sqrt{\mu^2-(q-F)^2}}^{\sqrt{\mu^2-(q-F)^2}} + \int_{b}^{\sqrt{\Lambda^2+M_{\rm q}^2}} \int_{-\sqrt{\Lambda^2+M_{\rm q}^2-q^2}}^{\sqrt{\Lambda^2+M_{\rm q}^2-q^2}} \right) \times q \left(\sqrt{p_3^2 + (q-F)^2} - \mu \right) dp_3\, dq.$$

If $F - \mu \leq M_{\rm q} \leq b \leq \sqrt{\Lambda^2 + M_{\rm q}^2} \leq F + \mu$,

$$\Phi_2(M, F, \mu) = \frac{3}{2\pi^2} \left(\int_{M_{\rm q}}^{b} \int_{-\sqrt{\mu^2-(q-F)^2}}^{\sqrt{\mu^2-(q-F)^2}} + \int_{b}^{\sqrt{\Lambda^2+M_{\rm q}^2}} \int_{-\sqrt{\Lambda^2+M_{\rm q}^2-q^2}}^{\sqrt{\Lambda^2+M_{\rm q}^2-q^2}} \right) \times q \left(\sqrt{p_3^2 + (q-F)^2} - \mu \right) dp_3\, dq.$$

If $F - \mu \leq b \leq M_{\rm q} \leq \sqrt{\Lambda^2 + M_{\rm q}} \leq F + \mu$,

$$\Phi_2(M, F, \mu) = \frac{3}{2\pi^2} \int_{M_{\rm q}}^{\sqrt{\Lambda^2+M_{\rm q}^2}} dq \int_{-\sqrt{\Lambda^2+M_{\rm q}^2-q^2}}^{\sqrt{\Lambda^2+M_{\rm q}^2-q^2}} dp_3\, q \left(\sqrt{p_3^2 + (q-F)^2} - \mu \right).$$

Here, b is the solution for q of the simultaneous equation:

$$p_3^2 + q^2 = \Lambda^2 + M_{\rm q}^2\,, \qquad p_3^2 + (q-F)^2 = \mu^2.$$

We were able to perform the integration over p_3, then define two functions for simplicity as follows:

$$\phi_1(q) \equiv \frac{3}{2\pi^2} q \left\{ -\mu\sqrt{\mu^2 - (F-q)^2} + (F-q)^2 \log\left(\frac{\mu + \sqrt{\mu^2 - (F-q)^2}}{|F-q|} \right) \right\},$$

$$\phi_2(q) \equiv \frac{3}{2\pi^2} q \left\{ \sqrt{\Lambda^2 + M_{\rm q}^2 - q^2} \left(-2\mu + \sqrt{F^2 + \Lambda^2 + M_{\rm q}^2 - 2Fq} \right) \right.$$
$$\left. + (F-q)^2 \log\left(\frac{\sqrt{F^2 + \Lambda^2 + M_{\rm q}^2 - 2Fq} + \sqrt{\Lambda^2 + M_{\rm q}^2 - q^2}}{|F-q|} \right) \right\}.$$

Using the above expressions, the final results are summarized as follows:

If $F - \mu \le M_{\rm q} \le F + \mu \le \sqrt{\Lambda^2 + M_{\rm q}^2}$,

$$\Phi_2(M, F, \mu) = \int_{M_{\rm q}}^{F+\mu} dq\, \phi_1(q). \tag{C2a}$$

If $M_{\rm q} \le F - \mu \le F + \mu \le \sqrt{\Lambda^2 + M_{\rm q}^2}$,

$$\Phi_2(M, F, \mu) = \int_{F-\mu}^{F+\mu} dq\, \phi_1(q). \tag{C2b}$$

If $M_{\rm q} \le F - \mu \le b \le \sqrt{\Lambda^2 + M_{\rm q}^2} \le F + \mu$,

$$\Phi_2(M, F, \mu) = \int_{F-\mu}^{b} dq\, \phi_1(q) + \int_{b}^{\sqrt{\Lambda^2+M_{\rm q}^2}} dq\, \phi_2(q). \tag{C2c}$$

If $F - \mu \le M_{\rm q} \le b \le \sqrt{\Lambda^2 + M_{\rm q}^2} \le F + \mu$,

$$\Phi_2(M, F, \mu) = \int_{M_{\rm q}}^{b} dq\, \phi_1(q) + \int_{b}^{\sqrt{\Lambda^2+M_{\rm q}^2}} dq\, \phi_2(q). \tag{C2d}$$

If $F - \mu \le b \le M_{\rm q} \le \sqrt{\Lambda^2 + M_{\rm q}} \le F + \mu$,

$$\Phi_2(M, F, \mu) = \int_{M_{\rm q}}^{\sqrt{\Lambda^2+M_{\rm q}^2}} dq \phi_2(q). \tag{C2e}$$

Finally, we discuss Φ_3 and Γ_3. We can derive the domain of integration easily in this case. The domain is re-expressed as

$$\Gamma_3 = \left\{ -\sqrt{\Lambda^2 + M_{\rm q}^2 - q^2} \le p_3 \le \sqrt{\Lambda^2 + M_{\rm q}^2 - q^2},\ M_{\rm q} \le q \le \sqrt{\Lambda^2 + M_{\rm q}^2} \right\}.$$

After integrating over p_3, we obtain the final result:

$$\Phi_3(M, F, \mu) = -\frac{3}{2\pi^2}\sum_{\eta}\int_{M_q}^{\sqrt{\Lambda^2+M_q^2}} dq\, q \left\{\sqrt{\Lambda^2+M_q^2-q^2}\sqrt{\Lambda^2+M_q^2+2\eta q F+F^2}\right.$$
$$\left. + (q+\eta F)^2 \log\left(\frac{\sqrt{\Lambda^2+M_q^2-q^2}+\sqrt{\Lambda^2+M_q^2+2\eta q F+F^2}}{|q+\eta F|}\right)\right\}. \quad \text{(C3)}$$

Appendix D. A possibility for the origin of the tensor-type interaction in the NJL model

In the QCD Lagrangian, the interaction part is written as

$$\mathcal{L}_{\rm int} = g\bar{\psi}(x)\,\gamma^{\mu}\psi(x)\,A_{\mu}(x), \quad \text{(D1)}$$

where $\psi(x)$ and $A_{\mu}(x)$ $(=A^a_{\mu}(x)T^a)$ are quark and gluon fields, respectively, and T^a represents the color $su(3)$ generators. Here, the two-gluon exchange diagrams are depicted in Fig. D1. These diagrams are obtained from the fourth-order perturbation of $\mathcal{L}_{\rm int}$:

$$\int d^4x\mathcal{L}_{\rm int}(x)\cdot\int d^4y\mathcal{L}_{\rm int}(y)\cdot\int d^4x\mathcal{L}_{\rm int}(x')\cdot\int d^4x\mathcal{L}_{\rm int}(y')$$
$$= g^4\int d^4x d^4y d^4x' d^4y'\bar{\psi}(x)\,\gamma^{\mu}\psi(x)\,A_{\mu}(x)\,\bar{\psi}(y)\,\gamma^{\nu}\psi(y)\,A_{\nu}(y)$$
$$\times\bar{\psi}(x')\,\gamma^{\rho}\psi(x')\,A_{\rho}(x')\,\bar{\psi}(y')\,\gamma^{\sigma}\psi(y')\,A_{\sigma}(y'). \quad \text{(D2)}$$

We here intend to describe the above expression as

$$\int d^4x\mathcal{L}_{\rm eff}, \quad \text{(D3)}$$

which should be expressed as the four-point interaction between quarks.

The processes in Figs. D1(a) and (b) may mainly be regarded as repeated processes of the one-gluon exchange process. Thus, we omit these processes in the contribution of the two-gluon exchange process. Therefore, let us first consider the diagram in Fig. D1(c). Writing the spinor indices, $i, j, \ldots$, explicitly, we contract the bilinear field, making the Feynman propagator

$$g^4\int d^4x d^4y d^4x' d^4y'\bar{\psi}_i(x)\,\gamma^{\mu}_{ij}\psi_j(x)\,A_{\mu}(x)\,\bar{\psi}_k(y)\,\gamma^{\nu}_{kl}\psi_l(y)\,A_{\nu}(y)$$
$$\times\bar{\psi}_m(x')\gamma^{\rho}_{mn}\psi_n(x')\,A_{\rho}(x')\,\bar{\psi}_p(y')\,\gamma^{\sigma}_{pq}\psi_q(y')\,A_{\sigma}(y')$$
$$\longrightarrow g^4\int d^4x d^4y d^4x' d^4y'\mathcal{L}_{(c)},$$
$$\mathcal{L}_{(c)} = -\bar{\psi}_i(x)\,\gamma^{\mu}_{ij}\bar{\psi}_k(y)\,\gamma^{\nu}_{kl}\gamma^{\rho}_{mn}\psi_n(x')\,\gamma^{\sigma}_{pq}\psi_q(y')$$
$$\times\langle\psi_j(x)\,\bar{\psi}_m(x')\rangle\langle A_{\mu}(x)\,A_{\sigma}(y')\rangle\langle\psi_l(y)\,\bar{\psi}_p(y')\rangle\langle A_{\nu}(y)\,A_{\rho}(x')\rangle. \quad \text{(D4)}$$

Here, it should be noted that the property of the Grassmann number for the fermion field is used. Thus, a minus sign appears. Here, $\langle\psi_i(x)\bar{\psi}_j(y)\rangle$ and $\langle A_{\mu}(x)A_{\nu}(y)\rangle$ $\left(=T^aT^b\langle A^a_{\mu}(x)A^b_{\nu}(y)\rangle\right)$

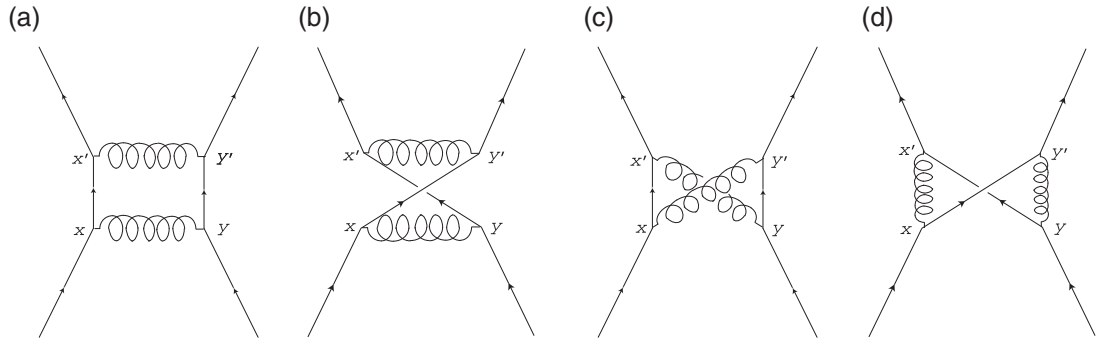

Fig. D1. Feynman diagrams of the two-gluon exchange process.

represent the Feynman propagators for quark and gluon fields, respectively:

$$\begin{aligned}\left\langle \psi_i\left(x\right)\bar{\psi}_j\left(y\right)\right\rangle &= \int \frac{d^4p}{i\left(2\pi\right)^4}\frac{\gamma^\mu p_\mu + M_q}{M_q^2 - p^2 - i\epsilon}e^{-ip(x-y)},\\ \left\langle A_\mu^a\left(x\right)A_\nu^b\left(y\right)\right\rangle &= \delta^{ab}\int \frac{d^4p}{i\left(2\pi\right)^4}\frac{1}{p^2+i\epsilon}\left[g_{\mu\nu} - \left(1-\alpha\right)\frac{p_\mu p_\nu}{p^2}\right]e^{-ip(x-y)},\end{aligned} \tag{D5}$$

where a and b are color indices, M_q is the quark mass, and α is a gauge parameter. Of course, the NJL model Lagrangian cannot be derived from QCD. Therefore, we have to give up the exact calculation. Thus, we assume the form of propagators so as to reproduce the four-point contact interaction between quarks. As for the quark propagator, the quark mass in the propagator is artificially set to a very large value or infinity:

$$\left\langle \psi_i(x)\,\bar{\psi}_j(y)\right\rangle \sim \int \frac{d^4p}{i\left(2\pi\right)^4}\frac{1_{ij}}{M_q}e^{-ip(x-y)} = \frac{1}{iM_q}\delta_{ij}\delta^4\left(x-y\right). \tag{D6}$$

As for the gluon propagator, a "gluon mass" M_g is artificially introduced and is taken as a very large value or infinity.

$$\begin{aligned}\left\langle A_\mu^a(x)\,A_\nu^b(y)\right\rangle &= \delta^{ab}\int \frac{d^4p}{i(2\pi)^4}\frac{1}{p^2+i\epsilon}\left[g_{\mu\nu} - \left(1-\alpha\right)\frac{p_\mu p_\nu}{p^2}\right]e^{-ip(x-y)}\\ &\to \delta^{ab}\int \frac{d^4p}{i\left(2\pi\right)^4}\frac{1}{p^2-M_g^2+i\epsilon}\left[g_{\mu\nu} - \left(1-\alpha\right)\frac{p_\mu p_\nu}{p^2}\right]e^{-ip(x-y)}\\ &\sim \delta^{ab}\int \frac{d^4p}{i\left(2\pi\right)^4}\frac{g_{\mu\nu}}{-M_g^2}e^{-ip(x-y)} = -\frac{1}{iM_g^2}\delta^{ab}g_{\mu\nu}\delta^4\left(x-y\right).\end{aligned} \tag{D7}$$

Hereafter, we denote $M_q^2M_g^4 \equiv M_{\rm eff}^6$, in which $M_{\rm eff}$ has mass dimension. Inserting the above "approximate" propagators into Eq. (D4), then, Eq. (D4) is rewritten as

$$\begin{aligned}\mathcal{L}_{(c)} = &\frac{C_2^2}{M_{\rm eff}^6}\bar{\psi}_i(x)\,\gamma_{ij}^\mu\gamma_{jn}^\rho\psi_n(x)\,\bar{\psi}_k(x)\,\gamma_{\rho,kl}\gamma_{\mu,lq}\psi_q(x)\\ &\times\delta^4\left(x-x'\right)\delta^4\left(x'-y\right)\delta^4\left(x-y'\right)\delta^4\left(y'-y\right),\end{aligned} \tag{D8}$$

where $C_2 = \sum_a T^a T^a$. Here, we again use the property of the Grassmann number. Thus, we obtain

$$g^4 \int d^4x d^4y d^4x' d^4y' \mathcal{L}_{(c)} = \frac{g^4 \delta^4(0)}{M_{\rm eff}^6} \cdot C_2^2 \int d^4x \; \bar{\psi}(x)\, \gamma^\mu \gamma^\rho \psi(x) \cdot \bar{\psi}(x)\, \gamma_\rho \gamma_\mu \psi(x)$$
$$= -g_T \int d^4x \bar{\psi}(x)\, \gamma^\mu \gamma^\nu \psi(x) \cdot \bar{\psi}(x)\, \gamma_\mu \gamma_\nu \psi(x)$$
$$+ 8 g_T \int d^4x \bar{\psi}(x)\, \psi(x) \cdot \bar{\psi}(x)\, \psi(x), \tag{D9}$$

where we define $g_T = g^4 \delta^4(0) C_2^2 / M_{\rm eff}^6$ (>0) and use $\gamma^\mu \gamma^\nu + \gamma^\nu \gamma^\mu = 2 g^{\mu\nu}$ and $\gamma^\mu \gamma_\mu = 4$. Here, $\delta^4(0) = \int d^4k/(2\pi)^4 \cdot e^{ik(x-y)}\big|_{x=y}$, which is regarded as a very large value or infinity in order to ensure that g_T has a finite value. Then, g_T has a dimension of $(\text{mass})^{-2}$.

Next, let us consider Fig. D1(d). As is similar to the case in Fig. D1(c), we obtain

$$g^4 \int d^4x d^4y d^4x' d^4y' \bar{\psi}_i(x)\, \gamma^\mu_{ij} \psi_j(x)\, A_\mu(x)\, \bar{\psi}_k(y)\, \gamma^\nu_{kl} \psi_l(y)\, A_\nu(y)$$
$$\times \bar{\psi}_m(x')\, \gamma^\rho_{mn} \psi_n(x')\, A_\rho(x')\, \bar{\psi}_p(y')\, \gamma^\sigma_{pq} \psi_q(y')\, A_\sigma(y')$$
$$\longrightarrow g^4 \int d^4x d^4y d^4x' d^4y' \mathcal{L}_{(d)},$$
$$\mathcal{L}_{(d)} = \bar{\psi}_i(x)\, \gamma^\mu_{ij} \bar{\psi}_k(y)\, \gamma^\nu_{kl} \gamma^\rho_{mn} \psi_n(x')\, \gamma^\sigma_{pq} \psi_q(y')$$
$$\times \langle \psi_l(y)\, \bar{\psi}_m(x') \rangle \langle A_\mu(x)\, A_\rho(x') \rangle \langle \psi_j(x)\, \bar{\psi}_p(y') \rangle \langle A_\nu(y)\, A_\sigma(y') \rangle. \tag{D10}$$

In order to obtain the four-point contact interaction for the NJL type, we "approximate" the propagators in (D6) and (D7). Then,

$$\mathcal{L}_{(d)} = \frac{C_2^2}{M_{\rm eff}^6} \bar{\psi}_i(x)\, \gamma^\mu_{ij} \gamma^\sigma_{jq} \psi_q(x)\, \bar{\psi}_k(x)\, \gamma_{\sigma,kl} \gamma_{\mu,ln} \psi_n(x)$$
$$\times \delta^4(x - x')\, \delta^4(x' - y)\, \delta^4(x - y')\, \delta^4(y' - y) \tag{D11}$$

is obtained. Therefore,

$$g^4 \int d^4x d^4y d^4x' d^4y' \mathcal{L}_{(d)} = \frac{g^4 \delta^4(0)}{M_{\rm eff}^6} \cdot C_2^2 \int d^4x \; \bar{\psi}(x)\, \gamma^\mu \gamma^\nu \psi(x) \cdot \bar{\psi}(x)\, \gamma_\nu \gamma_\mu \psi(x)$$
$$= -g_T \int d^4x \bar{\psi}(x)\, \gamma^\mu \gamma^\nu \psi(x) \cdot \bar{\psi}(x)\, \gamma_\mu \gamma_\nu \psi(x)$$
$$+ 8 g_T \int d^4x \bar{\psi}(x)\, \psi(x) \cdot \bar{\psi}(x)\, \psi(x). \tag{D12}$$

Finally, we obtain the effective Lagrangian density originating from the two-gluon exchange contribution between quarks, as illustrated in Fig. D2, as follows:

$$\int d^4x \mathcal{L}_{\rm eff} = g^4 \int d^4x d^4y d^4x' d^4y' \left(\mathcal{L}_{(c)} + \mathcal{L}_{(d)} \right)$$
$$= \int d^4x \left(-\frac{G_T}{4} \bar{\psi}(x) \gamma^\mu \gamma^\nu \psi(x) \cdot \bar{\psi}(x) \gamma_\mu \gamma_\nu \psi(x) + 2 G_T \bar{\psi}(x) \psi(x) \cdot \bar{\psi}(x) \psi(x) \right), \tag{D13}$$

where we define $G_T \equiv 8 g_T$, where $G_T > 0$. We take $G_T = 11\,\text{GeV}^{-2}$ in this paper. The first term corresponds to our tensor-type four-point interaction. Introducing the degree of freedom of the flavor,

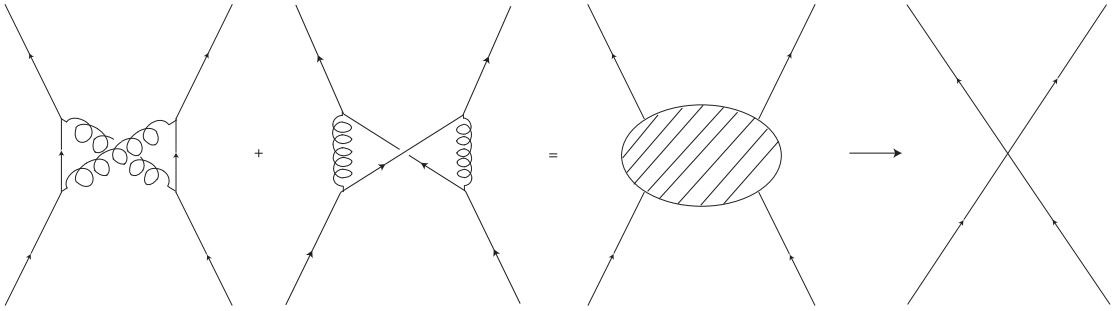

Fig. D2. Feynman diagrams of the two-gluon exchange process.

the tensor part is written as

$$\mathcal{L}_T = -\frac{G_T}{4}\left(\bar{\psi}\gamma^\mu\gamma^\nu\overrightarrow{\tau}\psi\right)\left(\bar{\psi}\gamma_\mu\gamma_\nu\overrightarrow{\tau}\psi\right), \tag{D14}$$

which is identical with the first term in Eq. (2.4). Of course, the above treatment is nothing but a crude approximation. Thus, we have to add another term so as to retain the chiral symmetry that the QCD has. The second term in Eq. (D13) represents the scalar–scalar interaction appearing in the original NJL model Lagrangian. However, the one-gluon exchange contribution may be washed out of this contribution by the two-gluon exchange.

References

[1] K. Fukushima and T. Hatsuda, Rep. Prog. Phys. **74**, 014001 (2011).
[2] M. G. Alford, A. Schmitt, K. Rajagopal, and T. Schafer, Rev. Mod. Phys. **80**, 1455 (2008) and references therein.
[3] M. Alford, K. Rajagopal, and F. Wilczek, Nucl. Phys. B **537**, 443 (1999).
[4] K. Iida and G. Baym, Phys. Rev. D **63**, 074018 (2001).
[5] L. McLerran and R. D. Pisarski, Nucl. Phys. A **796**, 83 (2007).
[6] E. Nakano and T. Tatsumi, Phys. Rev. D **71**, 114006 (2005).
[7] D. Nickel, Phys. Rev. Lett. **103**, 072301 (2009).
[8] M. Buballa and S. Carignano, Prog. Part. Nucl. Phys. **81**, 39 (2015) and references therein.
[9] Y. Tsue, J. da Providência, C. Providência, M. Yamamura, and H. Bohr, Prog. Theor. Exp. Phys. **2013**, 103D01 (2013).
[10] Y. Tsue, J. da Providência, C. Providência, M. Yamamura, and H. Bohr, Prog. Theor. Exp. Phys. **2015**, 013D02 (2015).
[11] Y. Tsue, J. da Providência, C. Providência, M. Yamamura, and H. Bohr, Prog. Theor. Exp. Phys. **2015**, 103D01 (2015).
[12] R. C. Duncan and C. Thompson, Astrophys. J. **392**, L9 (1992).
[13] C. Thompson and R. C. Duncan, Astrophys. J. **408**, 194 (1993).
[14] C. Thompson and R. C. Duncan, Astrophys. J. **473**, 322 (1996).
[15] Y. Tsue, J. da Providência, C. Providência, and M. Yamamura, Prog. Theor. Phys. **128**, 507 (2012).
[16] Y. Nambu and G. Jona-Lasinio, Phys. Rev. **122**, 345 (1961).
[17] Y. Nambu and G. Jona-Lasinio, Phys. Rev **124**, 246 (1961).
[18] T. Hatsuda and T. Kunihiro, Phys. Rep. **247**, 221 (1994).
[19] M. Buballa, Phys. Rep. **407**, 205 (2005).
[20] H. Bohr, P. K. Panda, C. Providência, and J. da Providência, Int. J. Mod. Phys. E **22**, 1350019 (2013).
[21] E. Nakano, T. Maruyama, and T. Tatsumi, Phys. Rev. D **68**, 105001 (2003).
[22] T. Tatsumi, T. Maruyama, and E. Nakano, Prog. Theor. Phys. Suppl. **153**, 190 (2004).
[23] M. Jaminon and E. Ruiz Arriola, Phys. Lett. B **443**, 33 (1998).
[24] M. Chizhov, JETP Lett. **80**, 73 (2004).
[25] E. J. Ferrer, V. de la Incera, I. Portillo, and M. Quiroz, Phys. Rev. D **89**, 085034 (2014).